Journal of Visualization, Vol. 5, No. 4 (2002) 355-361

Comparison of Sub-pixel Estimation of PIV Using Frequency Response Analysis

Okamoto, K.*

* Nuclear Engineering Research Laboratory, The University of Tokyo, Tokai-mura, Ibaraki 319-1188, Japan. e-mail: okamoto@utnl.jp

Received 23 November 2001.
Revised 26 April 2002.

***Abstract*:** The frequency responses on sub-pixel evaluation techniques have been investigated using the Monte-Carlo technique. The frequency response by the FFT based cross-correlation gives very good results although some gain loss does exist for small displacement (less than 0.5 pixel). Few gain losses are observed in the Direct Cross-Correlation, but the sub-pixel accuracy is limited to be about 0.1 pixel which implies that it could not detect a small displacement. To detect sub-pixel displacement with higher accuracy, the gradient technique with iterative correlation is the best. For a small interrogation area (e.g., 4×4), only the gradient technique can detect small displacement accurately.

***Keywords*:** PIV, sub-pixel estimation, cross-correlation, FFT, gradient technique.

1. Introduction

The Particle Image Velocimetry (PIV) is widely used to detect the quantitative characteristics of fluid flow. Currently, the turbulence structures are analyzed using the PIV results. The dynamic range of the PIV depends on the allowable maximum displacement of the particle and the detectable minimum displacement, i.e., sub-pixel estimation.

The error of the PIV evaluation is mainly classified into the erroneous vector and the error in sub-pixel estimation. The erroneous vector is caused by miss-tracking of the particle (pattern) movement. The error of the erroneous vector is usually larger than 1 pixel. Lots of error correction techniques, including iterative PIV (Raffel et al., 1999) and correlation multiplication (Hart, 2000), were proposed. The erroneous vectors may be removed easily, when the number of the vector is large enough while the sub-pixel error highly relates to image condition. The estimation technique determines the sub-pixel accuracy.

In this study, the sub-pixel estimation on the error is focused. The sub-pixel accuracy was also discussed by many researchers (Keane and Adrian, 1990; Westerweel et al., 1997; Raffel et al., 1999). They evaluated the peak locking, effects of out-of-plane and so on. To improve the sub-pixel accuracy, many techniques were proposed, including three-point Gaussian method. The image distortion techniques were also proposed (Lecordier et al., 1999). In the previous studies, the error on the PIV analysis was focused. The root mean square of the error was usually used for the index of the sub-pixel error. The RMS value is the integrated error, not showing the precise characteristics of error. For the turbulence analysis, the frequency responses of the PIV results are also very important. Although the RMS is small, the frequency responses may be bad in certain cases. Also the frequency responses relate to the extraction of spatial resolution. In this study, the frequency responses on the sub-pixel evaluation technique are investigated using the Monte-Carlo Simulation technique. The synthetic images are analyzed to estimate the frequency responses.

2. Evaluation Procedure

2.1 PIV Techniques

In this study, three PIV techniques are evaluated, i.e., the well-known FFT based cross-correlation technique (FFT) (Raffel et al., 1999), the direct cross-correlation (DCC) (Raffel et al., 1999) and gradient based technique with iterative correlation (Gradient) (Sugii et al., 2000). In FFT, no spatial offset is considered in the calculation of the covariant between the two images. Using the fixed interrogation area, the covariant of the two interrogations is calculated without any offset. In direct cross-correlation (DCC), the correlation coefficient is directly calculated considering the spatial offset. The difference between FFT and DCC is the consideration of the offset. For the sub-pixel estimation for the both techniques (FFT and DCC), the three-point Gaussian fitting method (Raffel et al., 1999) is applied. When the maximum cross-correlation value C was obtained at (i, j), the estimated sub-pixel displacement u in x-direction is expressed as follows,

$$u = i - \frac{1}{2}\frac{\ln C(i+1, j) - \ln C(i-1, j)}{\ln C(i+1, j) - 2\ln C(i, j) + \ln C(i-1, j)} \tag{1}$$

For the gradient technique with iteration correlation, initially the iterative cross-correlation is applied to detect the pixel-unit displacement. Since the gradient technique is not suitable for the larger displacement, the pixel displacement is estimated by cross-correlation technique. Then the sub-pixel displacement is detected using the gradient technique (Sugii et al., 2000). This technique is the hybrid technique between cross-correlation and gradient techniques.

$$u = \frac{\partial g / \partial t}{\partial g / \partial x} \tag{2}$$

where g is the intensity in the interrogation area.

To evaluate the frequency response on the PIV results, the synthetic images are generated according to the assumed velocity ***I***. Then, using the image, the velocity ***O***, was reconstructed by a PIV evaluation algorithm to obtain the transfer function ***O/I***. Figure 1 schematically shows the ***O/I*** responses. As shown in Fig. 1, the output response ***O/I*** contains the effects of image generator ***M/I***. The ideal condition is assumed for the image generator to avoid the effects of image generator. The following sinusoidal velocity (displacement) distributions are taken as the input velocity ***I***.

$$u = A\sin(2\pi f x + \phi) \tag{3}$$

With varying the amplitude A and the spatial frequency f, the output responses are evaluated. In this study, the velocity u and the frequency f are determined in the unit of pixel/interval and pixel^{-1}, respectively. In this study, the x-axis image size is set to be 1024 pixel. So, the spatial frequency f is determined as $f = k/1024$, where k is the number of waves in 1024 pixel. The certain phase delay ϕ is considered in the assumed velocity.

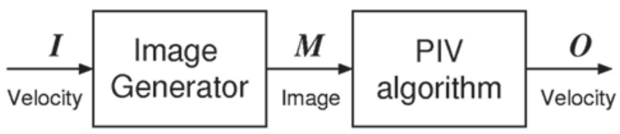

Fig. 1. Concept of the frequency response analysis.

2.2 Image Generator

As the image generator, the Gaussian particle image with random generator is used (Okamoto et al., 2000). The parameters are average particle size, standard deviation of particle size, laser light intensity distribution and number of particles. To generate the ideal image (***M/I*** $\cong$ 1), no noise and no out-of-plane motion are considered. The fill factor of the CCD is assumed to be 100%. The laser light sheet intensity distribution in the sheet thickness direction is assumed to be the Gaussian.

In this study, the particle size is fixed to be 2.0 pixel with standard deviation of 0.5 pixel. This means, the size of 80% particle is in the range of 1.5 to 2.5 pixel. Average number of particles is fixed to be 0.06/pixel ($N_I \approx$ in 32×32 interrogation area). The interrogation area is also fixed to be 32×32 for standard. Then, the number of particle in the interrogation area is about 60, which is large enough for the sub-pixel analysis for cross-correlation technique. In the gradient technique, the size of interrogation area implicitly is assumed to be odd number. Therefore, 33 × 33 interrogation area is applied for the gradient method. It is assumed to be few effects of small variation of the interrogation area on the results.

For comparison, very small interrogation area is also checked, i.e., 4 × 4. The number of particles in 4 × 4 is about 1, which is too small to detect the correct sub-pixel displacement. Example of the generated image is shown in Fig. 2, with the interrogation area size.

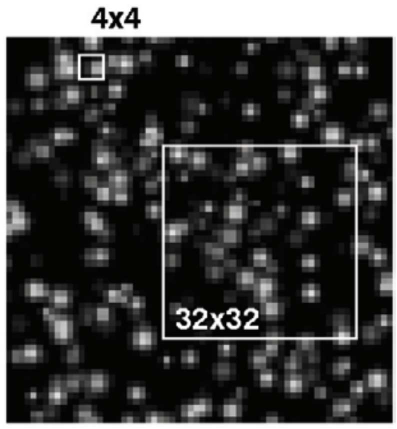

Fig. 2. Example of the generated images.

With applying the displacement in Eq. (3) to the individual particles, the second image is generated. Using the 1st and 2nd images, the displacement is reconstructed by these three PIV algorithms. The parameters of the transfer function are spatial frequency *f* and displacement amplitude *A*. The spatial frequency *f* is varied from 0.001 to 0.06 pixel^{-1}, i.e., 1 to 64 waves in 1024 pixel. To focus on the sub-pixel evaluation, the amplitude *A* was varied from 0.01 to 5 pixel. Fixed phase delay ($f_0 = 0.2$) is applied in Eq. (3).

3. Results and Discussion

3.1 Velocity Distributions

Figure 3 shows the example of the reconstructed velocity (displacement) for the lower frequency ($f = 0.002$ pixel^{-1}) and smaller amplitude ($A = 0.031$ pixel). The interrogation area is 32 × 32. Since there are no noises, the FFT can reconstruct such small amplitude fluctuation. However, the DCC has relatively larger errors. The gradient method can reconstruct the sub-pixel displacement much better than that of correlation techniques (FFT/DCC).

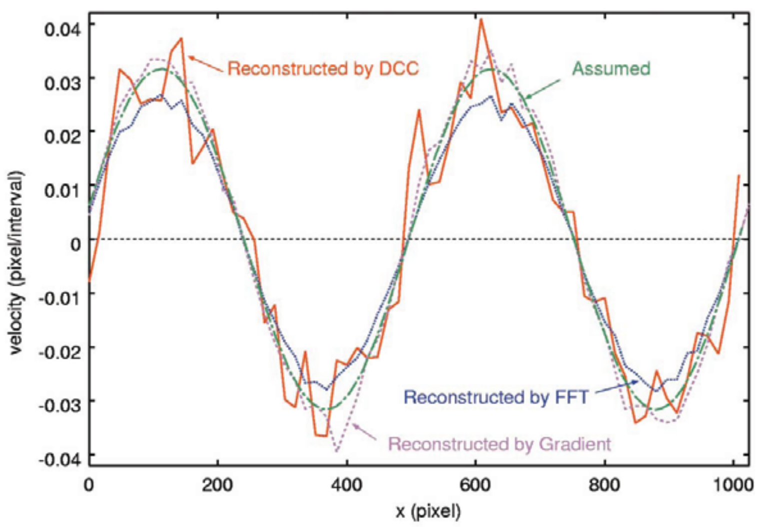

Fig. 3. Example of the reconstructed velocity distributions.

In the very small displacement case, the DCC has larger errors because of the follwing reasons. Although the cross-correlation value C at $x = 0$ is almost 1.0, the values at the neighbor ($x = -1$ and 1 pixel) contain lots of noise caused by the spatial offset, resulting in the relatively large errors for the sub-pixel evaluation. On the other hand, the FFT gives better results. The cross-correlation function with small displacement u could be expressed as the delta function $\delta(u)$, analytically. Especially in the small displacement case, the cross-correlation function will be a narrow Gaussian function, showing the correct reconstructions in FFT.

The reconstructed displacement (shown in Fig. 3) is estimated using the least square technique. The reconstructed displacement is fitted to a sinusoidal function, i.e., $u' = A' \sin(2\pi f x + \phi')$. The spatial frequency is set to be the assumed value. Then, the response amplitude A' and phase ϕ' are obtained with least square technique. The gain G is determined by the ratio of reconstructed amplitude to given amplitude, i.e., $G = A'/A$. Phase lag is the differences of phases, i.e., $\phi' - \phi$.

3.2 Bode Diagram

The Bode diagrams (gain response ($G = A'/A$) and phase lag ($\phi' - \phi$) for the three techniques are shown in Figs. 4 and 5. The red solid line denotes the theoretical response curve based on the sampling theory.

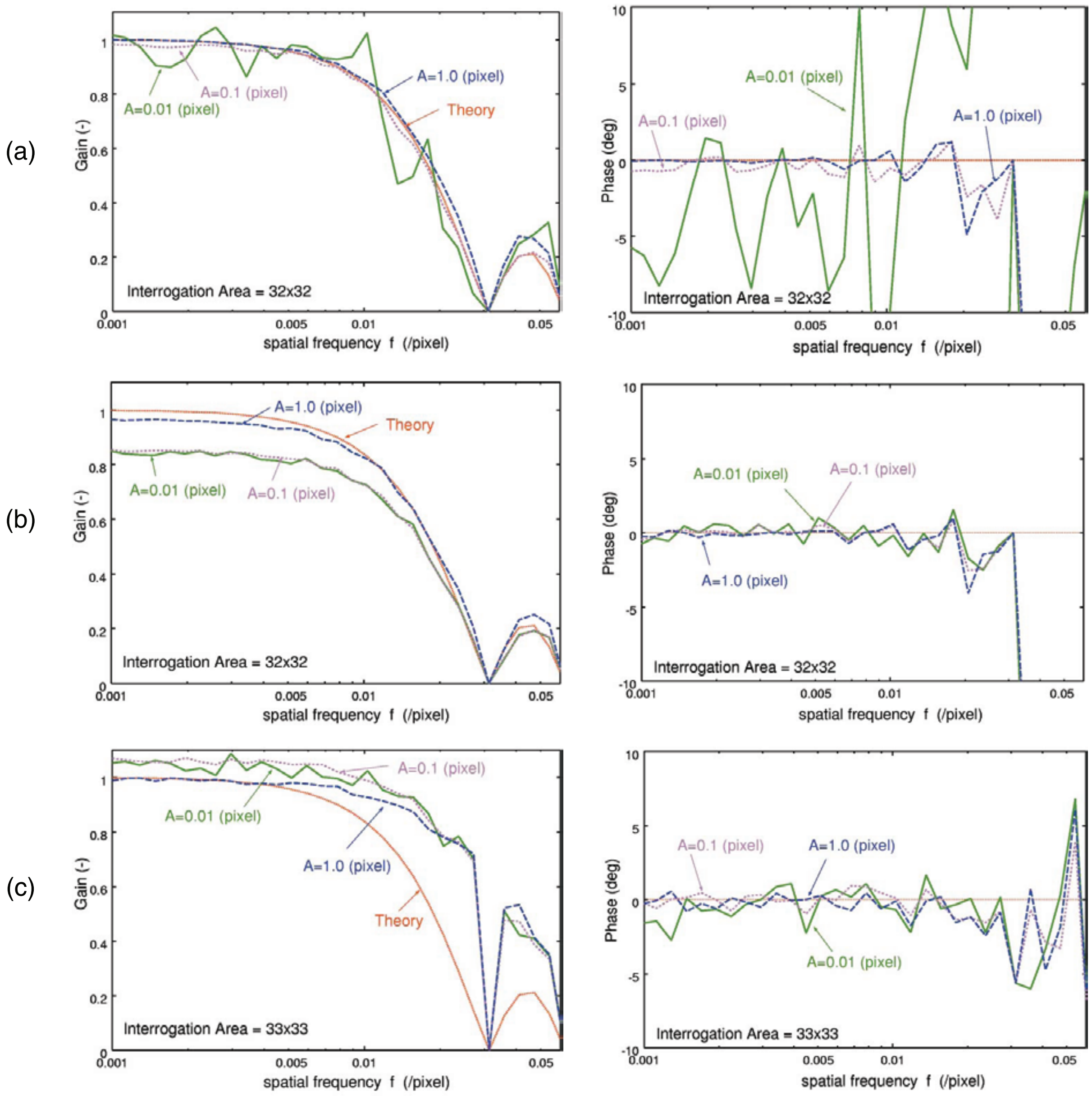

Fig. 4. Bode diagram for 32 × 32 interrogation. (a) Direct cross-correlation [DCC] (b) FFT cross-correlation (c) Gradient method with iteration

$$G = \frac{|\sin(\mathrm{p} f I)|}{\mathrm{p} f I} \tag{4}$$

where I is the interrogation area size, i.e., I = 32 and 4 for Figs. 4 and 5, respectively. The theoretical value denotes the maximum gain for the certain spatial frequency perturbations. In this study, the phase lag is used as the index of the reconstruction. The phase should be zero, when the reconstruction is correct.

In Fig. 4, the interrogation area size is 32 × 32, i.e., number of particles in the area (N_I) is about 60. For the DCC, the gain almost followed the theoretical one under the larger amplitude (A > 0.1 pixel). However, in smaller amplitude case (A = 0.01 pixel), it fluctuates because of the larger error. The phase information also supports the above results. Only the phases of larger amplitude cases are in the range of ±2 degree, showing good reconstruction. The DCC can reconstruct the velocity field correctly under larger amplitude case (A > 0.1 pixel).

Since the interrogation area is 32 pixel, the frequency larger than 1/32 (= 0.03) can not be detected according to the theoretical equation (Eq. (4)). For practical use, the 0.007 pixel^{-1} is the maximum frequency (G > 0.95). This means that the detectable fluctuation wavelength is larger than 120 pixel. However, usually much smaller fluctuation data were reported in some PIV analysis. As shown in Fig. 4, these data did have relatively

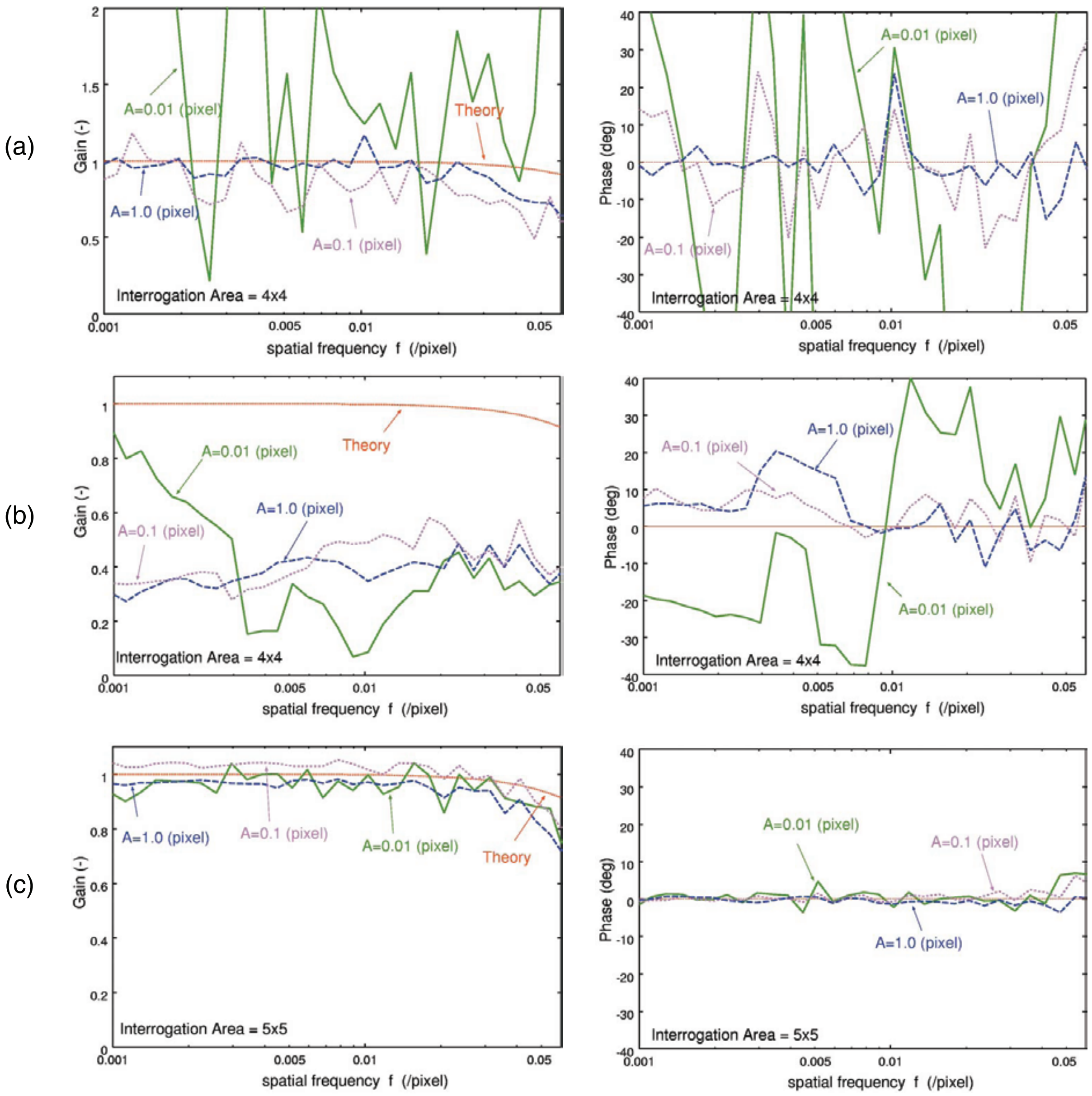

Fig. 5. Bode diagram for 4 × 4 interrogation. (a) Direct cross-correlation [DCC] (b) FFT cross-correlation (c) Gradient method with iteration

large gain loss. To detect high spatial frequency data, much smaller interrogation area is needed. The relationship between the theoretical gain and interrogation area should be taken into account for the measurement of PIV.

For the FFT, the gain losses (about 15%) were observed in the smaller amplitude ($A < 0.1$ pixel). In the larger case ($A = 1.0$ pixel), the gain almost agreed with the theoretical one. The estimated amplitude might be smaller than the real one under the smaller amplitude cases. This gain loss may relate to so called peak locking phenomena. On the other hand, they show very good phase responses even in the smaller amplitude cases, i.e., almost in the range of ±2 degree. No phase delay is observed in the FFT analysis.

For the Gradient method, the over responses (about 8%) are observed under the smaller amplitude ($A <$ 0.1 pixel). It almost is unity for the larger amplitude. The phase is distributed in the range of ±3 degree, showing the good reconstruction, even in the smaller amplitude cases.

All of the three techniques can reconstruct the fluctuation under the larger amplitude cases. Any technique can be applied with larger amplitude and smaller frequency fluctuation. When the amplitude is smaller ($A < 0.1$), DCC can not reconstruct the fluctuation. FTT and Gradient can reconstruct the fluctuation even in the smaller amplitude, however, the gain responses show the under and over estimation, respectively. The reconstruction of the smaller amplitude fluctuation should be more carefully evaluated. In these three techniques, the Gradient method is most superior for the estimation of the sub-pixel fluctuations.

4. Small Interrogation Area

In the recursive or iterative PIV technique, sometimes very small interrogation area might be used, e.g., 4×4. The smaller interrogation area shows the higher spatial frequency according to Eq. (4). Therefore, to improve the spatial resolution of PIV, the velocity data for the smaller interrogation area should be measured with high accuracy. The frequency responses on the size of interrogation area are evaluated in the case of 4×4 as shown in Fig. 5.

For the DCC, the gain curve fluctuates in the range of 0.8 to 1.2, even in the larger amplitude case. The phase also shows the larger fluctuation (up to 20 degree). Because of the smaller interrogation area, the Gaussian peak fit technique could not be applied. FFT was also out of applicable range. Only 16(= 4×4) pixels contribute to the cross-correlation calculation. The number is too small to detect the correct sub-pixel displacement.

However, the Gradient technique can reconstruct the flow field even in such a small interrogation area. The gain is distributed in the range of 10%. The phase also shows very good responses. Although the interrogation area of gradient technique is larger (5×5) than that of correlations (4×4), the gain and phase responses are much better than that of correlations. In the gradient technique, the displacement is calculated in every pixel, then it is estimated in the interrogation area using the least square technique. Therefore, the information of the whole images is directly used. The amount of the contributed information for sub-pixel estimation is considered to be much larger than that of FFT/DCC, resulting in the better sub-pixel accuracy.

This is the reason why the gradient technique is the best technique for the sub-pixel evaluation.

5. Amplitude Responses

To clarify the amplitude effects, the gain response curve is re-plotted as shown in Fig. 6. The *x*-axis denotes the amplitude. It is clearly seen that the responses by the FFT, DCC and Gradient technique are good under the relatively large amplitude cases ($A > 0.5$ pixel). The Gradient technique can reconstruct large amplitude cases, since it is a hybrid technique combined with the iterative correlation and gradient technique (Sugii et al., 2000). When the amplitude is less than 0.5 pixel, the gain decreases to be about 85% in FFT. It increases to be about 108% in Gradient. There exists a rapid recovery about 0.5 pixel displacement. The response in DCC is almost unity.

The responses for the small interrogation area cases are shown in Fig. 7. FFT and DCC show very bad responses. On the other hand, the Gradient technique shows very good responses for all amplitude cases. The Gradient technique is confirmed to give very good sub-pixel estimation, especially for small interrogation area.

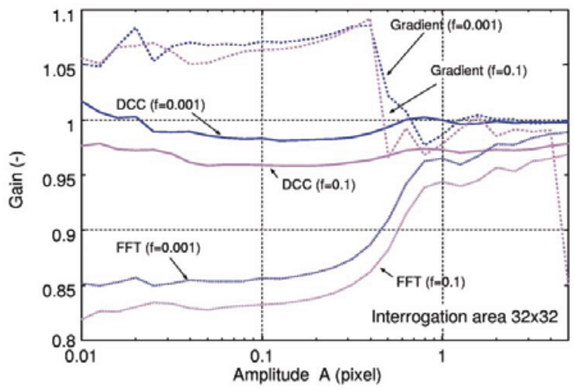

Fig. 6. Gain response with amplitude for large interrogation area (32 × 32).

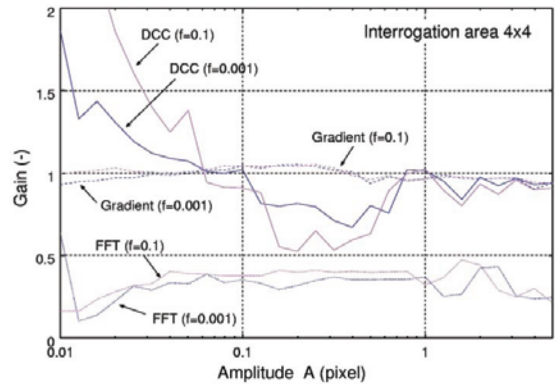

Fig. 7. Gain response with amplitude for small interrogation area (4 × 4).

6. Conclusion

The frequency response by the FFT based cross-correlation gives very good results although some gain loss does exist for small displacement (less than 0.5 pixel). Few gain losses are observed in the Direct Cross-Correlation, but the sub-pixel accuracy is limited to be about 0.1 pixel which implies that it could not detect a small displacement. The Gradient technique shows very good results even in the small amplitude case. In the small interrogation area, only the Gradient technique can be applied to estimate sub-pixel accuracy.

For the sub-pixel analysis, the Gradient technique should be applied, especially under the condition of small interrogation area and small displacement.

References

Hart, D. P., PIV Error Correction, Experiments in Fluids, 29 (2000), 13.

Keane, R. D. and Adrian, R. J., Optimization of Particle Image Velocimeters, Meas Sci Technol, 2 (1990), 1202.

Lecordier, B., Lecordier, J. C. and Trinite, M., Iterative Sub-pixel Algorithm for the Cross-correlation PIV Measurements, Proc. PIV-99, (1999), 37.

Okamoto, K., Nishio, S., Saga, T. and Kobayashi, T., Standard Images for Particle-image Velocimetry, Meas Sci Technol, 11 (2000), 685.

Raffel, M., Willert, C. and Kompenhans, J., Particle Image Velocimetry, (1999), Springer-Verlag.

Sugii, Y., Nishio, S., Okuno, Y. and Okamoto, K., A Highly Accurate Iterative PIV Technique Using a Gradient Method, Meas Sci Technol, 11 (2000), 1666.

Westerweel, J., Dabiri, D. and Gharib, M., The Effect of a Discrete Window Offset on the Accuracy of Cross-Correlation Analysis of Digital PIV Recordings, Exp Fluids, 23 (1997), 20.

Author Profile

Koji Okamoto: He received his M.Sc. (Eng) in Nuclear Engineering in 1985 from the University of Tokyo. He also received his Ph.D in Nuclear Engineering in 1992 from the University of Tokyo. He worked in Department of Nuclear Engineering, Texas A & M University as a visiting associate professor in 1994. He has been working in Nuclear Engineering Research Laboratory, the University of Tokyo as an associate professor since 1993. His research interests are Quantitative Visualization, PIV, Holographic PIV Flow Induced Vibration and Thermal-Hydraulics in Nuclear Power Plant.